JACS
JOURNAL OF THE AMERICAN CHEMICAL SOCIETY
pubs.acs.org/JACS
Article

Taming Inert B–H Bond with Low Energy Light: A Near-Infrared Light-Induced Approach to Facile Carborane Cluster-Amino Acid Coupling

Shengwen Xu, Hongjian Zhang, Jibo Zong, Houji Cao, Deshuang Tu,* Chang-sheng Lu,* and Hong Yan*

Cite This: J. Am. Chem. Soc. 2025, 147, 12845–12857
Read Online
ACCESS | Metrics & More | Article Recommendations | Supporting Information

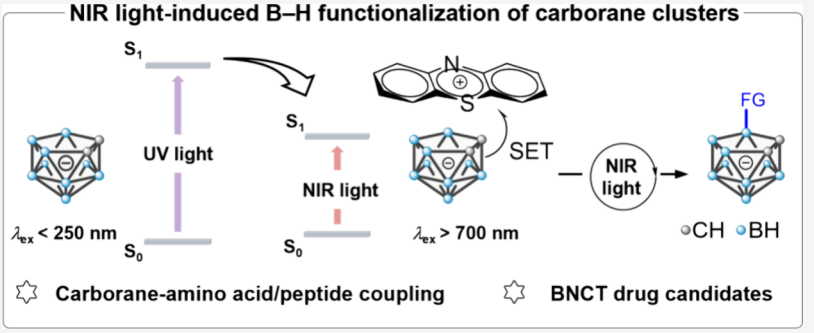

ABSTRACT: The selective functionalization of inert B–H bonds in carborane clusters has been a formidable challenge. Recent advances have witnessed such reactions through photoredox methods utilizing ultraviolet or visible light irradiation. However, high-energy light sources often suffer from poor energy efficiency, a limited substrate scope, undesired side reactions, and low scalability. Here, we present the first successful B–H bond functionalization under low-energy near-infrared (NIR) light using a carborane-based electron donor–acceptor complex. Both photophysical investigations and theoretical modeling reveal a facile single-electron transfer from the carborane cage to the electron-deficient photocatalyst, generating a carborane cage radical under NIR light irradiation. The follow-up radical pathway enables the direct coupling of carboranes with amino acids or oligopeptides, yielding a diverse array of carborane-functionalized amino acids or oligopeptides. Beyond expanding the known chemical space of boron cluster derivatives, we further demonstrate that carborane-based amino acids with imaging and targeting capabilities could serve as promising multifunctional boron carriers for boron neutron capture therapy. Thus, the selective B–H bond functionalization of the carboranes via NIR light not only provides a straightforward and practical strategy in boron cluster synthetic chemistry but also lays the foundation for the development of next-generation boron-containing biomolecules and advanced functional materials.

INTRODUCTION

The two-dimensional phenyl group is a fundamental structural motif in a wide range of chemicals, pharmaceutical compounds, and natural products. The recent advancements have focused on replacing the phenyl unit in bioactive compounds with three-dimensional bioisosteres,[1−4] such as adamantane,[2] bicyclo[1.1.1]pentane (BCP),[3] and cubane[4] to create novel drug molecules with enhanced biological activity (Figure 1a). Carborane clusters, a class of polyhedral boron clusters bearing three-dimensional aromaticity[5] and considered as boron-based bioisosteres of benzene, have been investigated in drug discovery,[6] exemplified by carborane-containing purinergic inhibitors.[6a] However, the direct and selective functionalization of B–H bonds in carboranes remains a significant challenge due to their inert nature and the chemical similarity of multiple B–H bonds on the boron cluster. This restricts the development of carborane-based drug candidates through B–H site modifications.

In the recent decade, significant progress has been made in the B–H functionalization of carboranes,[7−12] among which photoredox catalysis[13] was introduced as a new and powerful tool through the generation of boron cage radical intermediates. Strategies for generating boron-centered radicals have been developed via both preactivation of B–H bonds[14] and hydrogen atom transfer (HAT).[15] Notably, these methods have utilized ultraviolet (UV) or visible light (Figure 1b).

Received: January 25, 2025
Revised: March 20, 2025
Accepted: March 21, 2025
Published: April 1, 2025

https://doi.org/10.1021/jacs.5c01610
J. Am. Chem. Soc. 2025, 147, 12845–12857

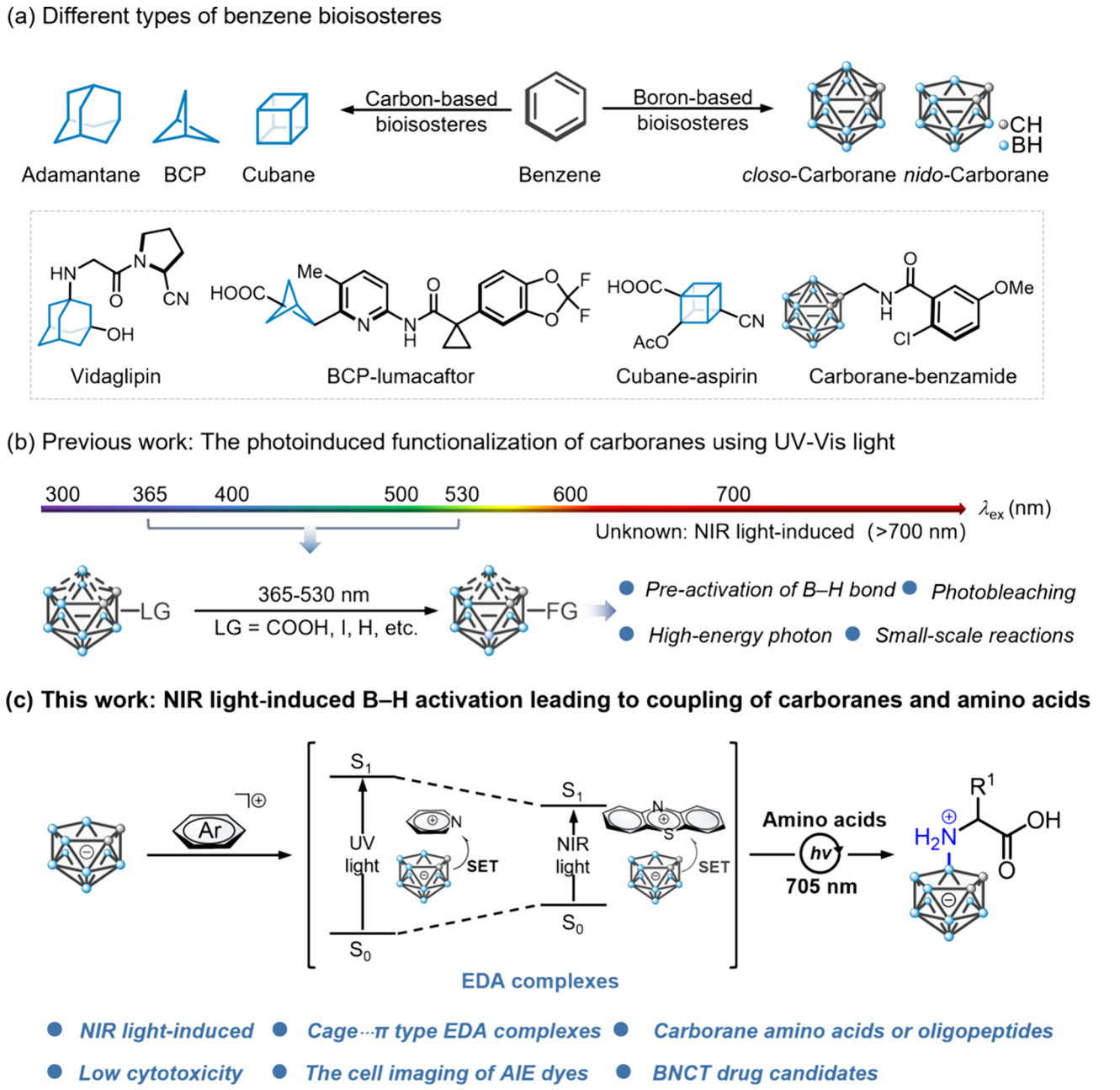

Figure 1. (a) Research background of benzene bioisosteres. (b) Known strategies of photoinduced B−H functionalization of carboranes. (c) This work: NIR light-induced direct coupling between *nido*-carboranes and amino acids or oligopeptides. The B−H−B bridging hydrogens of *nido*-carborane compounds have been omitted for clarity.

However, the use of high-energy photon irradiation may lead to undesirable side reactions, such as the photobleaching of substrates or products, and may not be compatible with biological molecules. Additionally, the penetration of UV/vis light through reaction media is limited, which poses challenges for large-scale preparation. To date, the use of low-energy photons, such as near-infrared (NIR) light, to initiate B−H activation of carboranes has not been reported. Since carborane clusters are photoinert species with no absorption longer than 250 nm, the development of NIR light-mediated B−H bond activation protocols requires innovative strategies.

On the other hand, it is well established that amino acids and their derivatives serve as fundamental building blocks with a wide range of applications in chemical synthesis, biomedicine, and functional materials. Undoubtedly, the functionalization of amino acids is important and applicable. The known carborane-based amino acid synthesis focused on the prefunctionalization of C−H bonds in the carborane clusters.[16] These methods are limited to carbon-substituted derivatives. Therefore, the development of a direct coupling methodology between carboranes and amino acids would be highly valuable for the creation of carborane-based pharmaceuticals and materials.

In this study, we demonstrate a strategy to utilize carborane-based electron donor−acceptor (EDA) complexes to achieve NIR-initiated B−H bond functionalization of *nido*-carboranes with amino acids and oligopeptides (Figure 1c). Within this framework, we designed and synthesized an array of carborane-

https://doi.org/10.1021/jacs.5c01610
J. Am. Chem. Soc. 2025, 147, 12845−12857

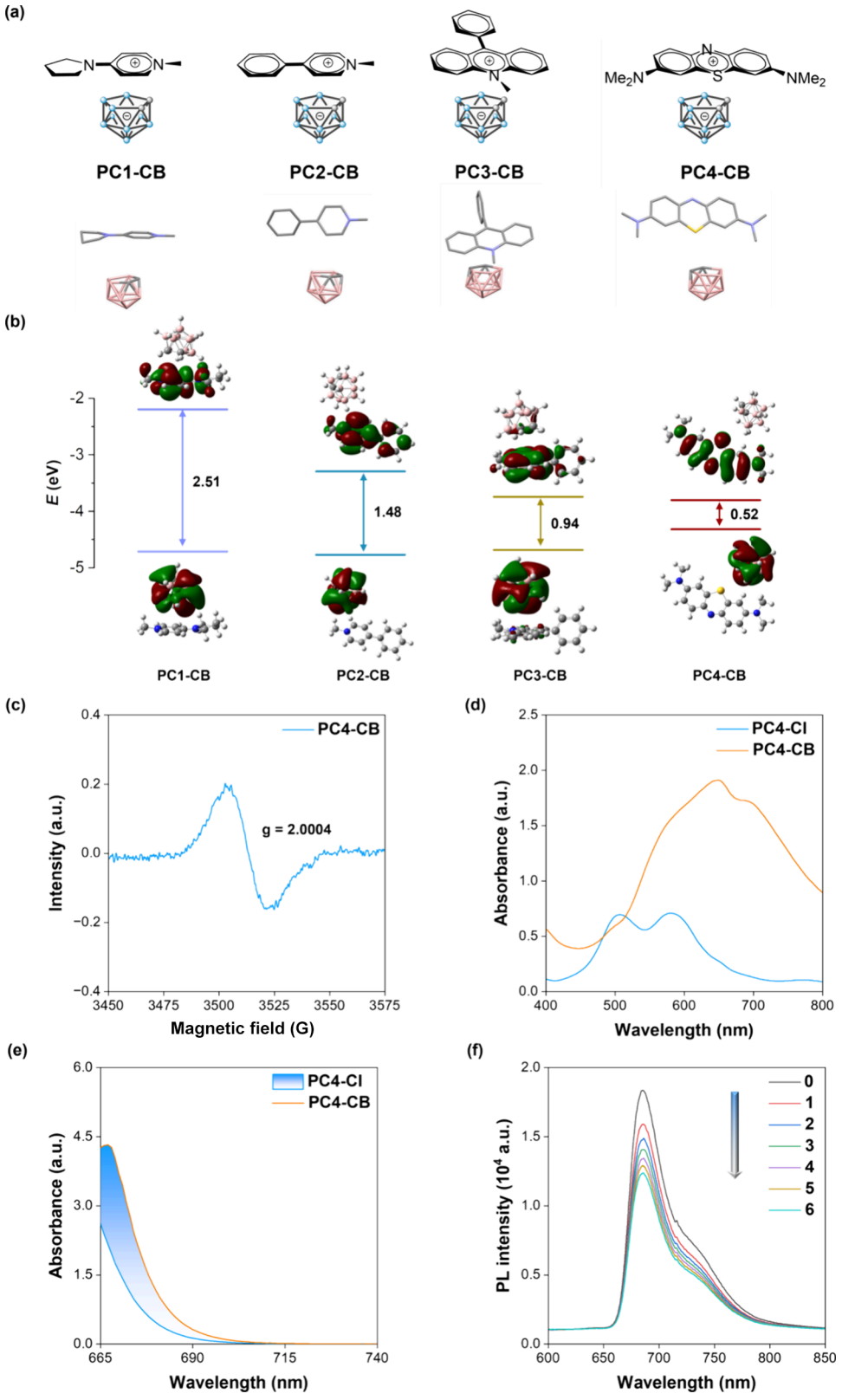

Figure 2. (a) Single-crystal structures of different EDA complexes. The B−H−B bridging hydrogen atoms in the EDA complexes and the single-crystal structures are omitted for clarity. (b) Theoretical calculations of energy gaps for different EDA complexes. (c) Electron paramagnetic resonance (EPR) spectrum of the **PC4-CB** EDA complex in the crystalline state. (d) UV/vis absorption spectra in the aggregated state for **PC4-Cl** and **PC4-CB**. (e) UV/vis absorption spectra in DCM (c = 0.1 mM) for **PC4-Cl** and **PC4-CB**. (f) Variable PL spectra of **PC4-Cl** in the presence of different molar ratios of *nido*-carborane in DCM (c = 10.0 μM).

based EDA complexes by selecting π-conjugated electron acceptors as photocatalysts with varying conjugation lengths and structures. Theoretical calculations indicate a significant reduction in the energy gap between the ground and excited

https://doi.org/10.1021/jacs.5c01610
J. Am. Chem. Soc. 2025, 147, 12845−12857

states with an increased conjugation length of the photocatalysts. Experimentally, in the case of the photocatalyst methylene blue (**PC4-Cl**), the generated carborane-based EDA complex undergoes a facile single-electron transfer (SET) process to produce the *nido*-carborane radical under NIR light excitation, which then proceeds the smooth follow-up coupling with amino acids or oligopeptides. Importantly, this reaction protocol takes place at room temperature by using an oxidant, O_2 in air, yielding up to 95%. Moreover, through the late-stage functionalization of products, we successfully synthesized new boron carriers bearing imaging and targeting properties for potential application in boron neutron capture therapy (BNCT). Thus, this work has established a new paradigm for the synthetic method of boron cluster chemistry and also opened a new avenue for the development of carborane-based therapeutic and imaging agents.

RESULTS AND DISCUSSION

Design of an NIR Light-Induced Reaction by Utilizing a Boron Cluster-Based EDA Complex. The NIR light-induced reactions have opened new horizons in synthetic chemistry due to the deep penetration and low photodamage.[17] However, carborane clusters are NIR light-inert species with an absorption less than 250 nm. To initiate the NIR light-induced B−H bond activation of carboranes, we introduced an engineered reaction system that utilizes EDA complexes. We have meticulously designed and synthesized a series of boron cluster-based EDA complexes by carefully screening the photocatalysts. These compounds feature electron-deficient π-conjugated aromatic rings that prefer to form the EDA interaction,[18] ranging from simple pyridinium derivatives (**PC1-CB** and **PC2-CB**) to larger conjugated systems such as acridinium (**PC3-CB**) and phenothiazinium (**PC4-CB**), as depicted in Figure 2a and Figure S2. The molecular structures were characterized by using nuclear magnetic resonance (NMR) spectroscopy, high-resolution mass spectrometry (HRMS), and single-crystal X-ray diffraction (SC-XRD) analysis. The crystallographic data reveal that all complexes exhibit offset or vertical stacking interactions between the aromatic rings and the C_2B_3 plane of *nido*-carborane, with bonding distances ranging from 4.1 to 5.2 Å. This arrangement indicates the presence of a cage···π interaction, aligning with previously reported findings.[18a] Density functional theory (DFT) calculations were conducted to elucidate the electronic properties of the synthesized EDA complexes (Figure 2b). The highest occupied molecular orbitals (HOMOs) are delocalized over the boron cage backbones, while the lowest unoccupied molecular orbitals (LUMOs) are predominantly localized on aromatic rings. The spatial separation suggests a strong charge-transfer character, which is anticipated to narrow the electronic band gap. Significantly, the extension of aromatic conjugation across the system results in a progressive reduction in the HOMO−LUMO energy gap. In the case of **PC4-CB**, the calculated energy gap is a mere 0.52 eV, indicating its feasibility by NIR light excitation. This finely tuned electronic structure not only underscores the strategic design of EDA complexes but also highlights the potential in NIR light-induced chemical transformations, offering a promising avenue for advancing photoredox catalysis in synthetic chemistry. The electron paramagnetic resonance (EPR) measurement of **PC4-CB** in the crystalline sample shows a clear signal (Figure 2c), verifying the facile SET process from the *nido*-carborane cage to phenothiazinium.

To further validate the computational results, photophysical measurements were performed. The UV/vis absorption spectrum of the **PC4-CB** complex in the aggregated state exhibits a pronounced red shift (~150 nm) relative to that of the parent **PC4-Cl**, thus showing absorption in the NIR region (Figure 2d). Such a huge redshift is attributed to the formation of a cage···π interaction, which facilitates the NIR light excitation. Comparable redshifts were also observed in the EDA complexes of **PC1-CB**, **PC2-CB**, and **PC3-CB**, as detailed in Figure S3. In contrast, **PC4-Cl** does not show absorption in the NIR region, highlighting the critical role of the cage···π interaction in contributing to NIR light excitation. In solution, **PC4-CB** also demonstrates an obvious red shift relative to that of **PC4-Cl** (Figure 2e). Further photoluminescence studies involved monitoring the fluorescence spectra of **PC4-Cl** (Figure 2f) by varying the ratios of *nido*-carborane in dichloromethane (DCM). The observed fluorescence weakening indicates electron transfer from the *nido*-carborane cage to phenothiazinium. These findings collectively verify a SET from the boron cage to the aromatic system both in the solid state and in solution, suggesting the potential for NIR light-induced reaction.

Table 1. Reaction Development

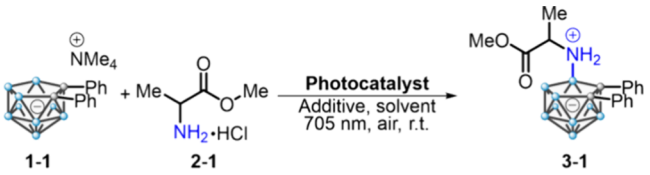

Entry	Cayalyst	Solvent	Additive	Yield (%)
1	**PC4-Cl**	DMSO	NH_4PF_6	0
2	**PC4-Cl**	CH_3OH	NH_4PF_6	0
3	**PC4-Cl**	DCM	NH_4PF_6	trace
4	**PC4-Cl**	Toluene	NH_4PF_6	trace
5	**PC4-Cl**	THF	NH_4PF_6	10
6	**PC4-Cl**	DME	NH_4PF_6	20
7	**PC4-Cl**	CH_3CN	NH_4PF_6	50
8[a]	**PC4-Cl**	CH_3CN/DCM	NH_4PF_6	82
9	**PC4-Cl**	CH_3CN/DCM	$NaHCO_3$	30
10	**PC4-Cl**	CH_3CN/DCM	NH_4F	40
11[b]	**PC4-Cl**	CH_3CN/DCM	NH_4PF_6	0
12	**PC1/2/3-BF$_4$**	CH_3CN/DCM	NH_4PF_6	0

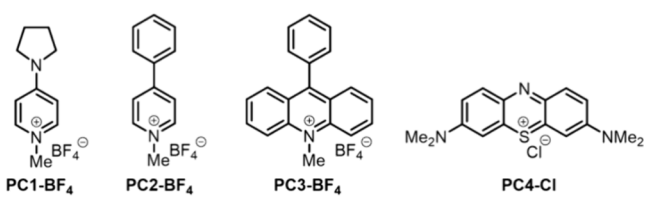

Reaction Development and Optimization. On the basis of the above insights gained from the photophysical measurements and computational studies, we initiated an investigation of the reactions between *nido*-carboranes and amino acid derivatives. The model reaction between $(NMe_4)(7,8\text{-}Ph_2\text{-}nido\text{-}C_2B_9H_{10})$ (**1−1**) and L-alanine methyl ester hydrochloride (**2−1**) was chosen under a variety of conditions.

https://doi.org/10.1021/jacs.5c01610
J. Am. Chem. Soc. 2025, 147, 12845−12857

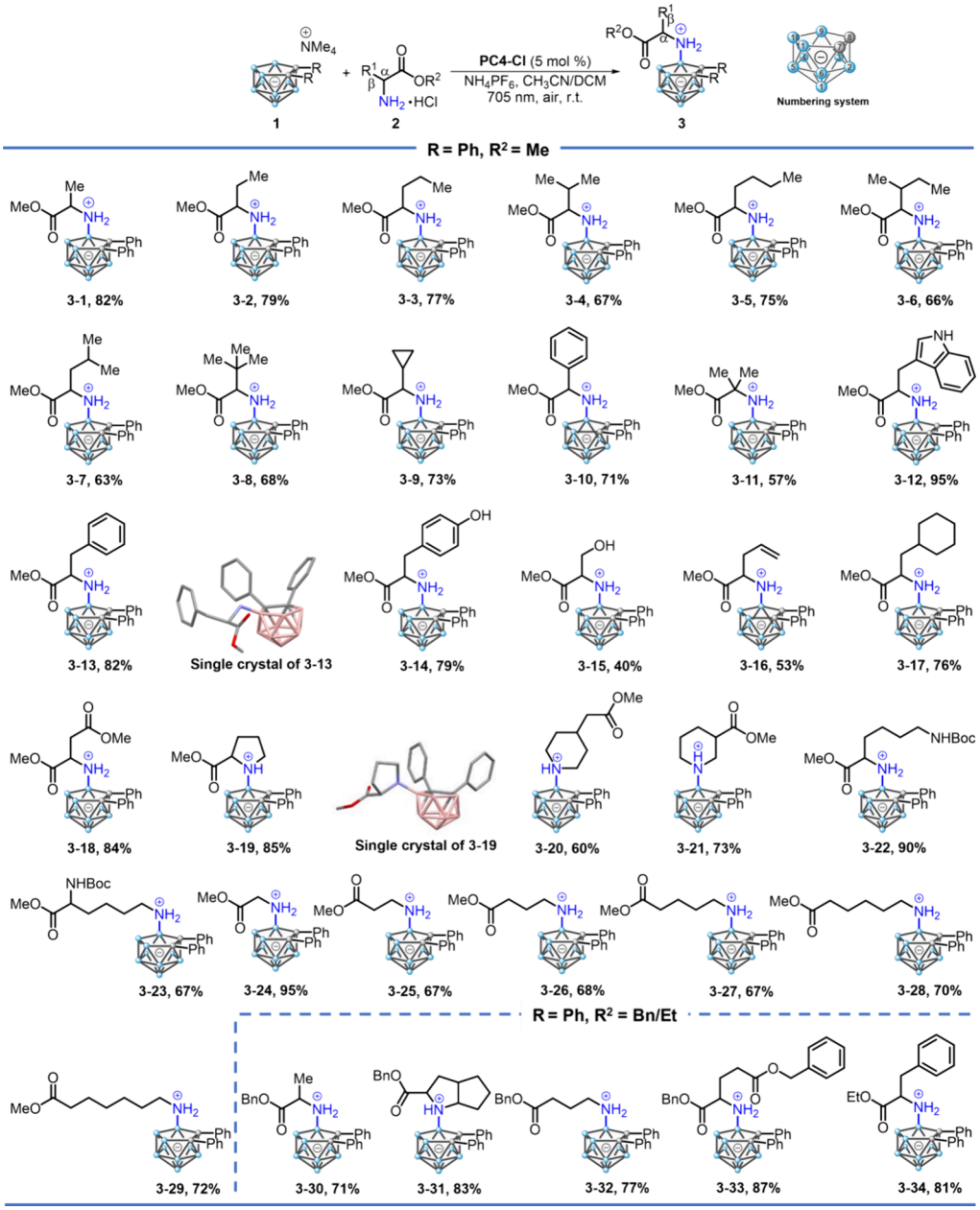

Figure 3. (a) **1**−**1** (0.1 mmol), **2** (0.2 mmol), **PC4-Cl** (5 mol %), NH_4PF_6 (0.1 mmol), DCM (1.0 mL), CH_3CN (1.0 mL), 12 W 705 nm LEDs, air, room temperature, 24 h, isolated yields. The B−H−B bridging hydrogen atoms in the products are omitted for clarity.

The careful screening progress of solvents revealed the necessity of a solvent mixture to obtain high yields. Single solvents such as dimethyl sulfoxide (DMSO), methanol (CH_3OH), dichloromethane (DCM), toluene, tetrahydrofuran (THF), 1,2-dimethoxyethane (DME), or acetonitrile (CH_3CN) resulted in diminished yields (Table 1, entries 1 to 7). The optimal solvent system was determined to be a 1:1 mixture of DCM and CH_3CN.

Table 1 (a) **1**−**1** (0.1 mmol), **2**−**1** (0.2 mmol), additive (0.1 mmol), photocatalyst (5 mol %), solvent (2.0 mL), 12 W 705 nm LEDs, air, room temperature, 24 h. (b) Without 12 W 705 nm LEDs. Isolated yields. The B−H−B bridging hydrogen atoms of the *nido*-carborane compounds are omitted for clarity.

The additive screening demonstrated that NH_4PF_6 is crucial, as alternative additives led to reduced yields (entries 9 and 10). The control experiments confirmed no reaction in the absence of NIR light irradiation (entry 11), emphasizing the necessity of NIR light activation. The photocatalyst evaluation indicated that **PC4-Cl** is the most effective catalyst for this transformation. Other photocatalysts lacking NIR absorption (Figure S3), such as 1-methyl-4-(pyrrolidin-1-yl)pyridin-1-ium tetrafluoroborate (**PC1-BF$_4$**), 1-methyl-4-phenylpyridin-1-ium tetrafluoroborate (**PC2-BF$_4$**), and 10-methyl-9-phenylacridin-10-ium tetrafluoroborate (**PC3-BF$_4$**), are ineffective under the same conditions (entry 12). Under the optimized conditions, i.e., 5 mol % **PC4-Cl**, NH_4PF_6 as an additive, DCM/CH_3CN solvent mixture, ambient air atmosphere, room temperature, and irradiation with 12 W NIR light LEDs for 24 h, the desired product **3**−**1** was obtained with an isolated yield of 82% (entry 8). Obviously, the coupling of *nido*-carborane with an amino acid derivative via B−H activation highlights the

https://doi.org/10.1021/jacs.5c01610
J. Am. Chem. Soc. 2025, 147, 12845−12857

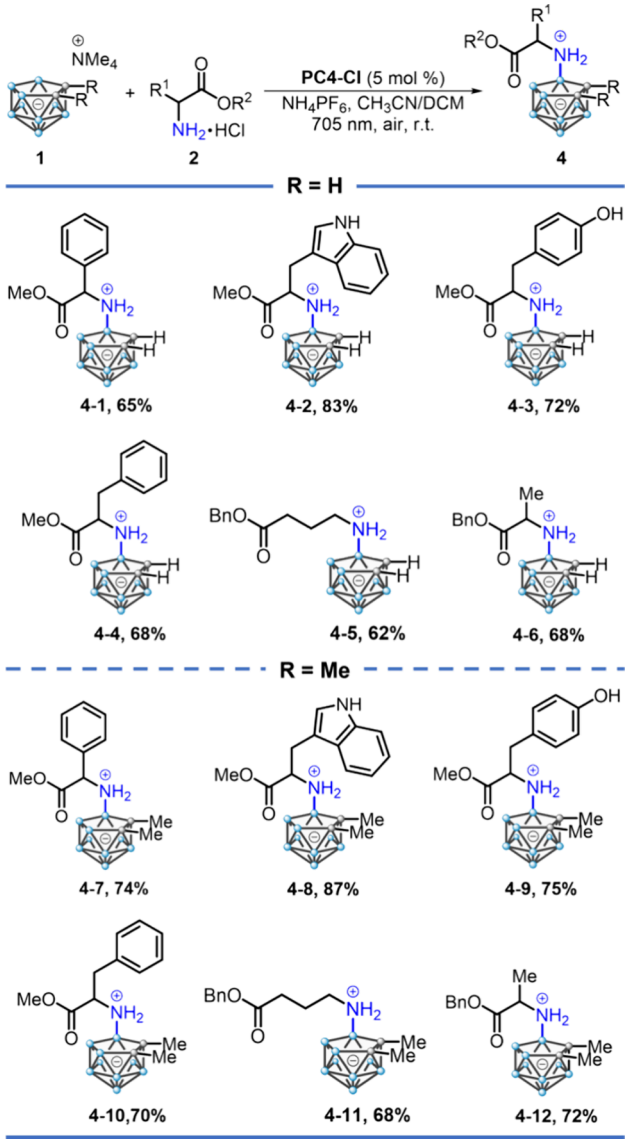

Figure 4. **1−2** or **1−3** (0.1 mmol), **2** (0.2 mmol), **PC4-Cl** (5 mol %), NH_4PF_6 (0.1 mmol), DCM (1.0 mL), CH_3CN (1.0 mL), 12 W 705 nm LEDs, air, room temperature, 24 h, isolated yields. The B−H−B bridging hydrogen atoms of the *nido*-carborane compounds are omitted for clarity.

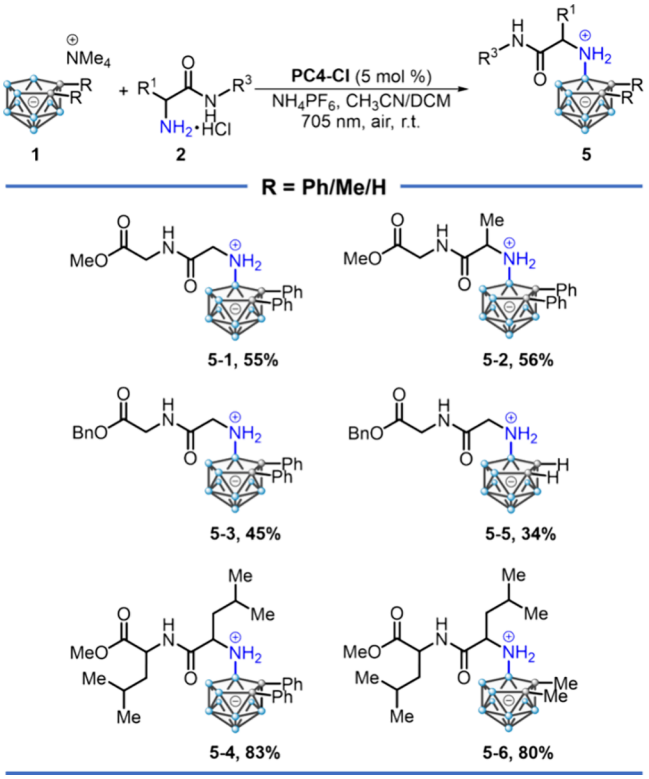

Figure 5. (a) **1−1**, **1−2**, or **1−3** (0.1 mmol), **2** (0.2 mmol), **PC4-Cl** (5 mol %), NH_4PF_6 (0.1 mmol), DCM (1.0 mL), CH_3CN (1.0 mL), 12 W 705 nm LEDs, air, room temperature, 48 h, isolated yields. The B−H−B bridging hydrogen atoms of the *nido*-carborane compounds are omitted for clarity.

efficacy of the **PC4-CB** EDA complex under NIR light irradiation.

Reaction Scope. Building upon the optimized experimental conditions, we explored the scope of the NIR light-induced coupling reaction between *nido*-carboranes (**1−1**, **1−2**, and **1−3**) and amino acid derivatives, as depicted in Figures 3 and 4. Our initial research focused on evaluating the impact of various R^1 substituents on the reactivities of the amino acid derivatives. Reactions involving primary, secondary, and tertiary alkyl groups, as well as a phenyl group at the α-carbon of the amino acids, proceeded smoothly under standard conditions, affording the corresponding products in moderate to good yields (63−82%, **3−1** to **3−10**). When two methyl groups are present at the α-carbon (**3−11**), a slightly decreased yield (57%) was observed, owing to the increased steric hindrance. We further extended the substrate scope by varying substituents at the β-carbon site of the amino acid derivatives. Surprisingly, an indole substituent at the β-position gave an excellent yield of 95% (**3−12**), highlighting the tolerance of reaction toward heteroaromatic systems and the potential for constructing biologically relevant molecules. Aromatic substituents at the β-position, such as phenyl and phenol, are compatible, delivering products in good yields of 82% (**3−13**) and 79% (**3−14**), respectively.

A gram-scale preparation of compound **3−13** led to an isolated yield of 72% (Figure S5). The reaction proceeded smoothly with the incorporation of hydroxyl (**3−15**), alkenyl (**3−16**), cyclohexyl (**3−17**), and ester group (**3−18**), yielding satisfactory results. Encouragingly, amino acid derivatives bearing cyclic alkyl groups on the nitrogen atom were well-tolerated, giving rise to yields ranging from 60% to 85% (**3−19** to **3−21**). The above results indicate that the steric hindrance at the β-carbon has a minimal effect on the reaction outcome.

Next, we investigated the reactivity of lysine derivatives with *nido*-carborane. The B−N coupling reactions proceeded efficiently, showing good to excellent yields (**3−22** and **3−23**). The extended methylene chains between the amino and ester functionalities (**3−24** to **3−29**) have no impact on the yield. We also examined the different R^2 groups, which exhibited a negligible effect on the yield (**3−30** to **3−34**). Furthermore, the substitutions at the C(7,8)-positions of the carborane cluster with hydrogens (**1−2**) or methyl groups (**1−3**) were equally applicable to the B−N coupling reaction (Figure 4), affording the expected products in good yields (**4−1** to **4−12**). These findings indicate the robustness and versatility of our method for the synthesis of carborane-amino acid conjugates.

https://doi.org/10.1021/jacs.5c01610
J. Am. Chem. Soc. 2025, 147, 12845−12857

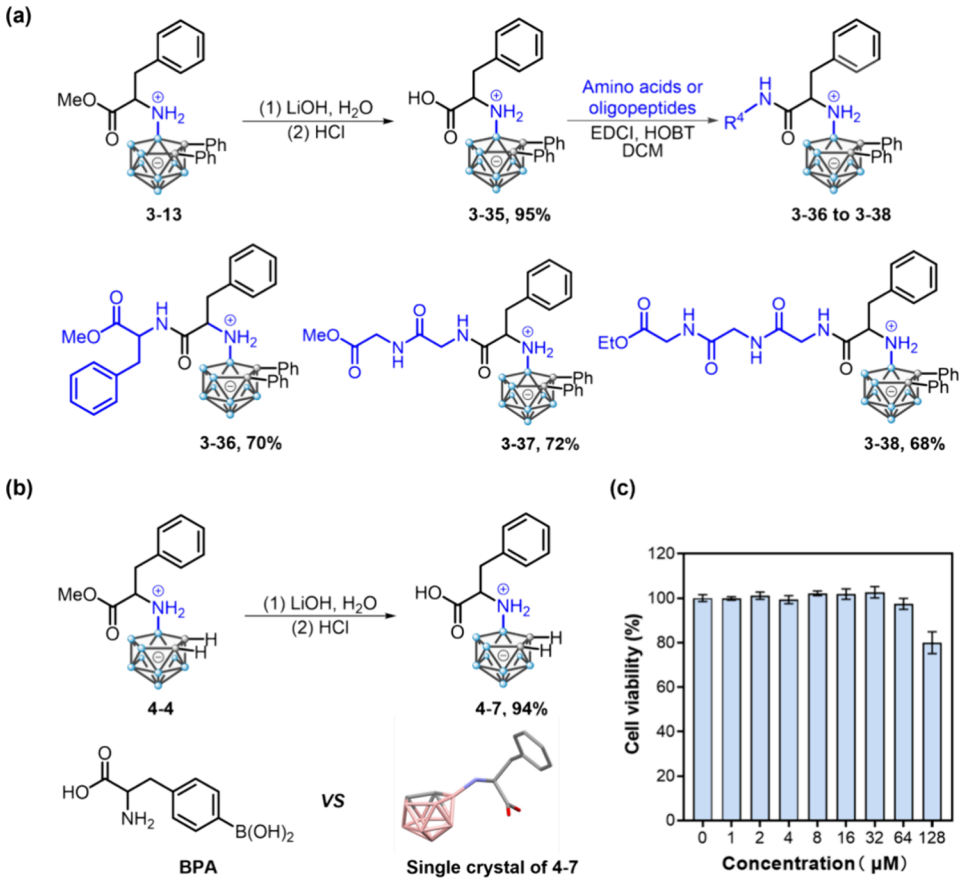

Figure 6. Synthetic applications. (a) Synthesis of carborane-based oligopeptides. (b) Molecular structures of carborane-based amino acid **4**−**7** vs the clinically used boron carrier **BPA**. (c) Test of PANC-1 cell viability of **4**−**7**. The B−H−B bridging hydrogen atoms in the products are omitted for clarity.

The above carborane-based amino acid products were carefully characterized by ^{1}H, ^{11}B, and ^{13}C NMR spectra and HRMS. The SC-XRD analysis of compounds **3**−**13** and **3**−**19**, unambiguously confirmed the exclusive site selectivity (Figure 3). To thoroughly assess the stability profile of the products, compound **3**−**13** was subjected to acidic and basic conditions, and the spectral changes were monitored using both ^{1}H NMR and ^{11}B NMR (Figures S6−S9). The compound exhibited exceptional chemical stability under neutral and acidic conditions. Under alkaline conditions, the bridging hydrogen can be removed, but it can be reversibly recovered upon acidification. In this manner, a deuterated carborane-based amino acid derivative (**D-3**−**13**) with the bridging hydrogen replaced by deuterium could be obtained (Figure S9).

Carborane-Oligopeptide Conjugation. Oligopeptides possess excellent cellular penetration and membrane permeability, rendering them promising candidates for therapeutic drug delivery systems.[19] In comparison to amino acids, the enhanced targeting capability and biological activity make oligopeptides particularly attractive as the targeting groups of boron carriers in the BNCT. Motivated by the successful coupling of *nido*-carboranes with amino acids, we extended our study to oligopeptides. Under standard reaction conditions but with a longer reaction time, we synthesized a series of carborane-oligopeptide conjugates (**5**−**1** to **5**−**6**) in satisfactory yields (Figure 5). The dipeptides such as Gly-Gly and Ala-Ala demonstrate good solubility, undergoing efficient coupling. However, tripeptides (e.g., Gly-Gly-Gly, <5% yield, Figure S10) or longer oligopeptides led to considerably diminished reaction efficiency owing to poor solubility.

Synthetic Applications. On the basis of the above findings, an alternative strategy was considered to obtain carborane-peptide conjugates with a longer-chain peptide. To address this issue, we first synthesized a carborane-based amino acid (i.e., **3**−**35**) by hydrolysis of **3**−**13** (Figure 6a and Figure S12). Subsequently, we performed a one-step condensation of **3**−**35** with other amino acids or oligopeptides. This approach gave satisfactory results, producing carborane-functionalized oligopeptides (**3**−**36** to **3**−**38**) with good yields (Figure 6a and Figure S13). This method suggests the potential for carboranes to be conjugated with polypeptides and even proteins and antibodies, thereby fulfilling the role of carboranes as benzene bioisosteres.

On the other hand, BNCT stands out as an advanced radiotherapy for the treatment of malignant tumors such as glioma, nasopharyngeal carcinoma, and melanoma, which needs both a boron carrier (or boron drug) and a neutron.[20] Currently, BNCT is facing the fact that it lacks suitable boron carriers as the clinically used boron carrier of 4-boron-L-phenylalanine[21] (**BPA**, Figure 6b) suffers from low solubility and stability under physiological conditions as well as low boron content. These limitations necessitate the development of novel boron carriers with enhanced solubility and stability and higher boron content. Amino acids, which are crucial for the rapid proliferation of cancer cells, have been explored as targeting units in drug design. In this study, a library of

https://doi.org/10.1021/jacs.5c01610
J. Am. Chem. Soc. 2025, 147, 12845−12857

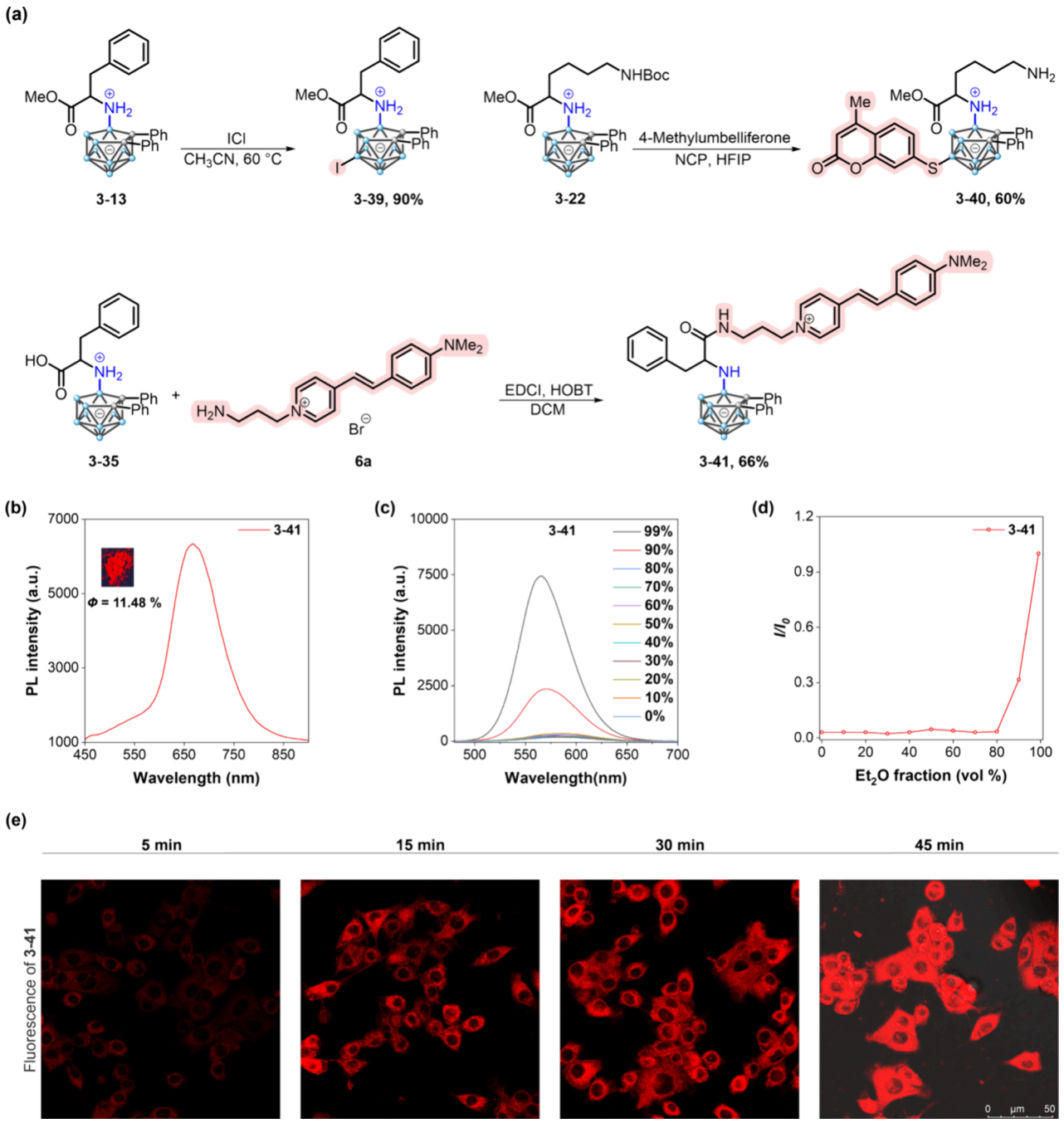

Figure 7. (a) Modular synthesis of new BNCT drug candidates. The B−H−B bridging hydrogen atoms of the *nido*-carborane compounds are omitted for clarity. (b) PL spectrum in the aggregated state for **3−41**. (c) PL spectra in CH_3OH/Et_2O mixtures with different Et_2O fractions (f) for **3−41** (c = 10 μM, λ_{ex} = 450 nm), demonstrating an AIE property. (d) Plot of the relative emission intensity (I/I_0) versus Et_2O fraction; I_0 and I are the peak values of PL intensities of **3−41**. (e) Cell (mouse 4T1) imaging of **3−41** at different times.

carborane-based amino acids has been synthesized which are anticipated as potential boron carriers for BNCT. Along this line, compound **4−7** was chosen as a representative example owing to its structural similarity to **BPA** (Figure 6b). Distinct from **BPA**, it exhibits excellent solubility in water (15 mg/mL), which is over 20 times higher than **BPA** because of its zwitterionic nature. It also shows extremely high stability under acidic and physiological conditions (Figures S6 and S7). Additionally, it demonstrates low cytotoxicity toward human pancreatic cancer cells (PANC-1), even in the concentration of 64 μM (Figure 6c and Figure S14). These properties, in combination with its higher boron content, make it a promising candidate for BNCT and other pharmaceutical applications.

Next, we introduced imaging functionality to carborane-based amino acids through the late-stage modification of compounds **3−13** and **3−22** (Figure 7a). Utilizing our recently reported method based on dative bond activation,[10b] two compounds of **3−39** and **3−40** were synthesized via a one-step electrophilic substitution. Notably, the iodine radionuclides (such as ^{124}I and ^{125}I) could be similarly introduced as in compound **3−39** for biomedical imaging in disease diagnosis[22] (Figure 7a and Figure S15). Additionally, coumarin derivatives are a class of fluorescent dyes with potential

https://doi.org/10.1021/jacs.5c01610
J. Am. Chem. Soc. 2025, 147, 12845−12857

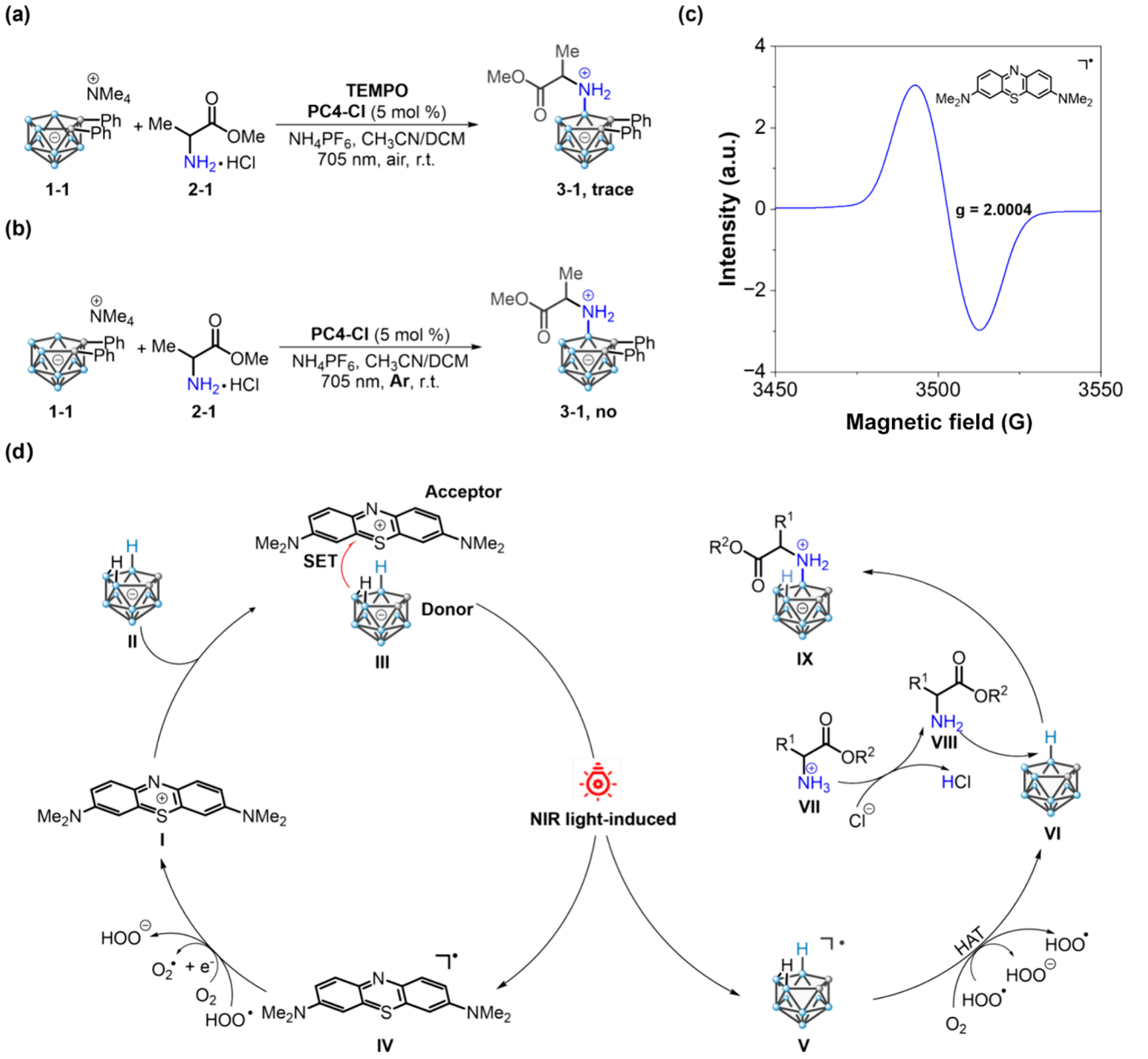

Figure 8. (a) Radical capture experiment. (b) Validation of oxygen participation. The B−H−B bridging hydrogen atoms of the *nido*-carborane compounds are omitted for clarity. (c) EPR signal of the phenothiazine radical. (d) Proposed reaction mechanism.

applications in biomedical imaging and sensing. In **3−40**, the coumarin group has been incorporated as an imaging group (Figure 7a and Figure S16). The two compounds have integrated three essential factors such as a boron cluster as a pharmacophore, targeting unit, and imaging group, thus making them more promising candidates for the next generation of boron carriers for BNCT.

Moreover, the AIE (aggregation-induced emission)-active luminogens represent a type of promising species for bioimaging and diagnostics[23] and have evident advantages over traditional fluorescent dyes. As such, we designed and synthesized carborane-based AIE-active luminogen **3−41** by one-step condensation of **3−35** with fluorescent compound **6a** (Figure 7a and Figure S18). We meticulously investigated the photophysical properties (Figure 7b−d and Figure S19) and cellular bioimaging capability of **3−41**. Its solid-state luminescence quantum efficiency is 11.48% (Figure 7b). The brighter cellular bioimaging in the 4T1 cells (mouse breast cancer cells) is shown with an extension of time owing to the AIE property (Figure 7e and Figure S20). Compound **3−41** might have potential in cancer diagnosis and treatment in BNCT.

Mechanistic Studies. To gain a profound understanding of the reaction mechanism, we undertook a series of experiments. First, the addition of 2,2,6,6-tetramethylpiperidine-1-oxyl (TEMPO) to the standard reaction system led to the formation of only a trace amount of product (Figure 8a and Figure S21), suggesting the involvement of a radical process. Conducting the reaction under an Ar atmosphere resulted in no product (Figure 8b and Figure S22). The electron paramagnetic resonance (EPR) technique was utilized to detect the radical intermediates in the reaction system. The phenothiazine radical signal was observed with a *g*-value of 2.0004 (Figure 8c and Figure S23), consistent with the literature report.[24] We have previously reported *nido*-carborane radical with a lifetime of approximately 2.5 μs using the

https://doi.org/10.1021/jacs.5c01610
J. Am. Chem. Soc. 2025, 147, 12845−12857

transient EPR technique.[18a] Based on the above mechanistic studies and literature reports,[18a,24] we propose the following reaction mechanism (Figure 8d). Initially, the EDA complex (**III**) is formed through the cage···π interaction between the phenothiazine cation (**I**) of the photocatalyst and the *nido*-carborane anion (**II**). Upon NIR light irradiation, a SET occurs, leading to the generation of a phenothiazine radical (**IV**) and the *nido*-carborane cage radical (**V**). In air, the *nido*-carborane radical (**V**) undergoes a bridging hydrogen atom transfer (HAT) to generate an active boron cage intermediate (**VI**). This intermediate then reacts with a nucleophilic reagent, such as an amino acid derivative or oligopeptide, to yield the functionalized carborane derivative (**IX**) at the electron-deficient B(9/11) site. Note that the Hirshfeld charge analysis reveals that the B(9/11) sites of intermediate (**VI**) possess higher charge values than the B(10) site (Table S2), indicating their greater propensity for nucleophilic reactions. In addition, the synergetic hydrogen transfer from B(9/11)−H to regenerate the bridging hydrogen is another driving force for selective substitution. The phenothiazine radical (**IV**) can be oxidized by oxygen in air or hydroperoxy radicals to regenerate the cation (**I**), thereby completing the catalytic cycle.

CONCLUSIONS

We developed a novel strategy utilizing an EDA complex to achieve inert B−H functionalization of carborane clusters by NIR light excitation. Interestingly, the common methylene blue can serve as the photocatalyst to form a novel EDA complex with *nido*-carborane. Such an EDA complex can facilitate a facile SET upon NIR light irradiation to create the reactive carborane cage radical, which further leads to the coupling with amino acids or oligopeptides. This approach shows broad substrate scope, high efficiency (up to 95% yield), exclusive regioselectivity at the B(9/11) site, as well as the uniqueness of the use of air as an oxidant to promote the transformation of active carborane radical. Through the late-stage modification of the carborane-based amino acid products, an array of novel carborane-based peptides and BNCT drug candidates have been synthesized. This overcomes the limitations of the clinically used boron carrier **BPA**, which lacks imaging capability and has low boron content and low solubility. Overall, this study presents a groundbreaking paradigm to diversify boron clusters by coupling with biological molecules under extremely simple and mild conditions and explores their potential applications.

ASSOCIATED CONTENT

Supporting Information

The Supporting Information is available free of charge at https://pubs.acs.org/doi/10.1021/jacs.5c01610.

Experimental details, synthetic procedures, characterization data, crystallographic data, and mechanistic studies of this article (PDF)

Accession Codes

Deposition Numbers 2406309, 2406311−2406315, and 2406317 contain the supplementary crystallographic data for this paper. These data can be obtained free of charge via the joint Cambridge Crystallographic Data Centre (CCDC) and Fachinformationszentrum Karlsruhe Access Structures service.

AUTHOR INFORMATION

Corresponding Authors

Deshuang Tu − *State Key Laboratory of Coordination Chemistry, Jiangsu Key Laboratory of Advanced Organic Materials, School of Chemistry and Chemical Engineering, Nanjing University, Nanjing 210023, China*; Email: tudeshuang@126.com

Chang-sheng Lu − *State Key Laboratory of Coordination Chemistry, Jiangsu Key Laboratory of Advanced Organic Materials, School of Chemistry and Chemical Engineering, Nanjing University, Nanjing 210023, China*; Email: luchsh@nju.edu.cn

Hong Yan − *State Key Laboratory of Coordination Chemistry, Jiangsu Key Laboratory of Advanced Organic Materials, School of Chemistry and Chemical Engineering, Nanjing University, Nanjing 210023, China*; orcid.org/0000-0003-3993-0013; Email: hyan1965@nju.edu.cn

Authors

Shengwen Xu − *State Key Laboratory of Coordination Chemistry, Jiangsu Key Laboratory of Advanced Organic Materials, School of Chemistry and Chemical Engineering, Nanjing University, Nanjing 210023, China*

Hongjian Zhang − *State Key Laboratory of Coordination Chemistry, Jiangsu Key Laboratory of Advanced Organic Materials, School of Chemistry and Chemical Engineering, Nanjing University, Nanjing 210023, China*

Jibo Zong − *State Key Laboratory of Coordination Chemistry, Jiangsu Key Laboratory of Advanced Organic Materials, School of Chemistry and Chemical Engineering, Nanjing University, Nanjing 210023, China*

Houji Cao − *School of Chemistry and Chemical Engineering, Henan Normal University, Xinxiang, Henan 453007, China*; orcid.org/0000-0002-0539-9124

Complete contact information is available at: https://pubs.acs.org/10.1021/jacs.5c01610

Notes

The authors declare no competing financial interest.

ACKNOWLEDGMENTS

This work is supported by the National Natural Science Foundation of China (92261202, 22401141 and 22201067), the Natural Science Foundation of Jiangsu Province (BZ2022007 and BK20241229), the Fundamental Research Funds for the Central Universities (2024300362), Henan Normal University, the TaiShan Industrial Experts Programme, and the high-performance computing center of Nanjing University.

REFERENCES

(1) For selected reviews and book of the bioisosteres, see: (a) Patani, G. A.; LaVoie, E. J. Bioisosterism: A Rational Approach in Drug Design. *Chem. Rev.* **1996**, *96*, 3147−3176. (b) Brown, N., Ed. *Bioisosteres in Medicinal Chemistry*; John Wiley & Sons, 2012; Vol. *54*.

(2) Wanka, L.; Iqbal, K.; Schreiner, P. R. The Lipophilic Bullet Hits the Targets: Medicinal Chemistry of Adamantane Derivatives. *Chem. Rev.* **2013**, *113*, 3516−3604.

(3) (a) Garry, O. L.; Heilmann, M.; Chen, J. J.; Liang, Y. F.; Zhang, X. H.; Ma, X. S.; Yeung, C. S.; Bennett, D. J.; MacMillan, D. W. C. Rapid Access to 2-Substituted Bicyclo[1.1.1]pentanes. *J. Am. Chem. Soc.* **2023**, *145*, 3092−3100. (b) Zhang, X. H.; Smith, R. T.; Le, C.; McCarver, S. J.; Shireman, B. T.; Carruthers, N. I.; MacMillan, D. W.

C. Copper-mediated Synthesis of Drug-like Bicyclopentanes. *Nature* **2020**, *580*, 220−226. (c) Frank, N.; Nugent, J.; Shire, B. R.; Pickford, H. D.; Rabe, P.; Sterling, A. J.; Zarganes-Tzitzikas, T.; Grimes, T.; Thompson, A. L.; Smith, R. C.; Schofield, C. J.; Brennan, P. E.; Duarte, F.; Anderson, E. A. Synthesis of *meta*-Substituted Arene Bioisosteres from [3.1.1]propellane. *Nature* **2022**, *611*, 721−726.

(4) (a) Nagasawa, S.; Hosaka, M.; Iwabuchi, Y. *ortho*-C−H Acetoxylation of Cubane Enabling Access to Cubane Analogues of Pharmaceutically Relevant Scaffolds. *Org. Lett.* **2021**, *23*, 8717−8721. (b) Tsien, J.; Hu, C.; Merchant, R. R.; Qin, T. Three-dimensional Saturated C(sp^3)-rich Bioisosteres for Benzene. *Nat. Rev. Chem.* **2024**, *8*, 605−627. (c) Cuadros, S.; Paut, J.; Anselmi, E.; Dagousset, G.; Magnier, E.; Dell'Amico, L. Light-Driven Synthesis and Functionalization of Bicycloalkanes, Cubanes and Related Bioisosteres. *Angew. Chem., Int. Ed.* **2024**, *63*, No. e202317333.

(5) (a) Grimes, R. N. *Carboranes*. 3rd ed.; Academic Press: Amsterdam, 2016. (b) Hosmane, N. S.; Eagling, R. D. *Handbook of Boron Science: With Applications in Organometallics, Catalysis, Materials and Medicine*; World Scientific: London, 2018. (c) Solà, M. Aromaticity Rules. *Nat. Chem.* **2022**, *14*, 585−590.

(6) For selected reviews and references of the carborane bioisosteres, see: (a) Wilkinson, S. M.; Gunosewoyo, H.; Barron, M. L.; Boucher, A.; McDonnell, M.; Turner, P.; Morrison, D. E.; Bennett, M. R.; McGregor, I. S.; Rendina, L. M.; Kassiou, M. The First CNS-Active Carborane: A Novel $P2X_7$ Receptor Antagonist with Antidepressant Activity. *Acs. Chem. Neurosci.* **2014**, *5*, 335−339. (b) Stockmann, P.; Gozzi, M.; Kuhnert, R.; Sárosi, M. B.; Hey-Hawkins, E. New Keys for Old Locks: Carborane-containing Drugs as Platforms for Mechanism-based Therapies. *Chem. Soc. Rev.* **2019**, *48*, 3497−3512. (c) Issa, F.; Kassiou, M.; Rendina, L. M. Boron in Drug Discovery: Carboranes as Unique Pharmacophores in Biologically Active Compounds. *Chem. Rev.* **2011**, *111*, 5701−5722. (d) Marfavi, A.; Kavianpour, P.; Rendina, L. M. Carboranes in Drug Discovery, Chemical Biology and Molecular Imaging. *Nat. Rev. Chem.* **2022**, *6*, 486−504. (e) Tse, E. G.; Houston, S. D.; Williams, C. M.; Savage, G. P.; Rendina, L. M.; Hallyburton, I.; Anderson, M.; Sharma, R.; Walker, G. S.; Obach, R. S.; Todd, M. H. Nonclassical Phenyl Bioisosteres as Effective Replacements in a Series of Novel Open-Source Antimalarials. *J. Med. Chem.* **2020**, *63*, 11585−11601. (f) Li, H.; Gao, Y. L.; Ma, J. J. Advances in Nonclassical Phenyl Bioisosteres for Drug Structural Optimization. *Future Med. Chem.* **2022**, *14*, 1681−1692. (g) Jena, B. B.; Pattanayak, M. R. *Carborane Clusters for Promoting Medicinal Applications*. Apple Academic Press: New Forms of Carbon: 2024; pp 219248. (h) Gruzdev, D. A.; Levit, G. L.; Krasnov, V. P.; Charushin, V. N. Carborane-Containing Amino Acids and Peptides: Synthesis Properties and Applications. *Coord. Chem. Rev.* **2021**, *433*, No. 213753.

(7) For selected reviews of *o*-carborane, see: (a) Bregadze, V. I. Dicarba-*closo*-Dodecaboranes $C_2B_{10}B_{12}$ and Their Derivatives. *Chem. Rev.* **1992**, *92*, 209−223. (b) Olid, D.; Nunez, R.; Vinas, C.; Teixidor, F. Methods to Produce B−C, B−P, B−N and B−S Bonds in Boron Clusters. *Chem. Soc. Rev.* **2013**, *42*, 3318−3336. (c) Zhang, X. L.; Yan, H. Transition Metal-induced B−H Functionalization of *o*-Carborane. *Coord. Chem. Rev.* **2019**, *378*, 466−482. (d) Qiu, Z. Z.; Xie, Z. W. A Strategy for Selective Catalytic B−H Functionalization of *o*-Carboranes. *Acc. Chem. Res.* **2021**, *54*, 4065−4079.

(8) For selected references of *o*-carborane, see: (a) Herberhold, M.; Yan, H.; Milius, W.; Wrackmeyer, B. Rhodium-induced Selective B(3)/B(6)-Disubstitution of *ortho*-Carborane-1,2-Dithiolate. *Angew. Chem., Int. Ed.* **1999**, *38*, 3689−3691. (b) Qiu, Z. Z.; Quan, Y. J.; Xie, Z. W. Palladium-Catalyzed Selective Fluorination of *o*-Carboranes. *J. Am. Chem. Soc.* **2013**, *135*, 12192−12195. (c) Zhang, X. L.; Zheng, H. M.; Li, J.; Xu, F.; Zhao, J.; Yan, H. Selective Catalytic B−H Arylation of *o*-Carboranyl Aldehydes by a Transient Directing Strategy. *J. Am. Chem. Soc.* **2017**, *139*, 14511−14517. (d) Baek, Y.; Cheong, K.; Ko, G. H.; Han, G. U.; Han, S. H.; Kim, D.; Lee, K.; Lee, P. H. Iridium-catalyzed Cyclative Indenylation and Dienylation through Sequential B(4)−C Bond Formation, Cyclization, and Elimination from *o*-Carboranes and Propargyl Alcohols. *J. Am. Chem. Soc.* **2020**, *142*, 9890−9895. (e) Mills, H. A.; Martin, J. L.; Rheingold, A. L.; Spokoyny, A. M. Oxidative Generation of Boron-Centered Radicals in Carboranes. *J. Am. Chem. Soc.* **2020**, *142*, 4586−4591. (f) Guo, C.; Zhang, J.; Ge, Y.; Qiu, Z. Z.; Xie, Z. W. Asymmetric Palladium Migration for Synthesis of Chiral-at-Cage *o*-Carboranes. *Angew. Chem., Int. Ed.* **2025**, *64*, No. e202416987. (g) Cao, H. J.; Chen, M.; Sun, F. X.; Zhao, Y.; Lu, C. S.; Zhang, X. L.; Shi, Z. Z.; Yan, H. Variable Metal Chelation Modes and Activation Sequence in Pd Catalyzed B−H Poly-arylation of Carboranes. *ACS. Catal.* **2021**, *11*, 14047−14057. (h) Ma, Y. N.; Gao, Y.; Ma, Y. B.; Wang, Y.; Ren, H. Z.; Chen, X. N. Palladium-Catalyzed Regioselective B(9)-Amination of *o*-Carboranes and *m*-Carboranes in HFIP with Broad Nitrogen Sources. *J. Am. Chem. Soc.* **2022**, *144*, 8371−8378. (i) Ma, Y. N.; Ren, H. Z.; Wu, Y. X.; Li, N.; Chen, F. J.; Chen, X. N. B(9)-OH-*o*-Carboranes: Synthesis, Mechanism, and Property Exploration. *J. Am. Chem. Soc.* **2023**, *145*, 7331−7342. (j) Sun, M.; Feng, L.; Lu, J. Y. Breaking the Base Barrier: Cu (II)-Mediated C−H Heteroarylation of *o*-Carboranes with Base-Sensitive Heteroaryl Halides. *Org. Lett.* **2024**, *26*, 3697−3702. (k) Hamdaoui, M.; Liu, F.; Cornaton, Y.; Lu, X. Y.; Shi, X. H.; Zhang, H.; Liu, J. Y.; Spingler, B.; Djukic, J. P.; Duttwyler, S. An Iridium-Stabilized Borenium Intermediate. *J. Am. Chem. Soc.* **2022**, *144*, 18359−18374. (l) Yang, H. B.; Guo, Y.; Cao, K.; Jiang, Q. J.; Teng, C. C.; Zhu, D. Y.; Wang, S. H. Iridium-catalyzed Selective Arylation of B(6)−H of 3-Aryl-*o*-Carboranes with Arylboronic Acid via Direct B−H Activation. *Chem. Commun.* **2024**, *60*, 1124−1127.

(9) For selected references of nucleophilic substitution on *nido*-carboranes, see: (a) Tutusaus, O.; Teixidor, F.; Nuñez, R.; Viñas, C.; Sillanpää, R.; Kivekäs, R. Recent Studies on RR'S·$C_2B_9H_{11}$ Charge-Compensated Ligands: Crystal Structures of 10-($S(CH_3)_2$)-7,8-$C_2B_9H_{11}$ and 10-($S(CH_2)_4$)-7,8-$C_2B_9H_{11}$. *J. Organomet. Chem.* **2002**, *657*, 247−255. (b) Frank, R.; Adhikari, A. K.; Auer, H.; Hey-Hawkins, E. Electrophile-Induced Nucleophilic Substitution of the *nido*-Dicar-Baundecaborate Anion *nido*-7,8-$C_2B_9H_{12}^-$ by Conjugated Heterodienes. *Chem. Eur. J.* **2014**, *20*, 1440−1446. (c) Stogniy, M. Y.; Erokhina, S. A.; Suponitsky, K. Y.; Anisimov, A. A.; Sivaev, I. B.; Bregadze, V. I. Nucleophilic Addition Reactions to the Ethylnitrilium Derivative of *nido*-Carborane 10-EtC≡N-7,8-C2B9H11. *New J. Chem.* **2018**, *42*, 17958−17967.

(10) For selected references of electrophilic substitution on *nido*-carboranes, see: (a) Frank, F.; Grell, T.; Hiller, M.; Hey-Hawkins, E. Electrophilic Substitution of *nido*-Dicarbaborate Anion 7,8-*nido*-$C_2B_9H_{12}^-$ with Sulfenyl Chlorides. *Dalton Trans.* **2012**, *41*, 6155−6161. (b) Ren, H.; Zhou, N.; Ma, W.; Zhang, P.; Tu, D.; Lu, C. S.; Yan, H. Dative Bonding Activation Enables Precise Functionalization of the Remote B−H Bond of *nido*-Carborane Clusters. *J. Am. Chem. Soc.* **2024**, *146*, 26543−26555.

(11) For selected references of oxidative substitution on *nido*-carboranes, see: (a) Yang, Z. M.; Zhao, W. J.; Liu, W.; Wei, X.; Chen, M.; Zhang, X.; Zhang, X. L.; Liang, Y.; Lu, C. S.; Yan, H. Metal-Free Oxidative B−N Coupling of *nido*-Carborane with N−Heterocycles. *Angew. Chem., Int. Ed.* **2019**, *58*, 11886−11892. (b) Chen, M.; Zhao, D.; Xu, J.; Li, C.; Lu, C.; Yan, H. Electrooxidative B−H Functionalization of *nido*-Carboranes. *Angew. Chem., Int. Ed.* **2021**, *60*, 7838−7844.

(12) For selected references of metal mediation for *nido*-carboranes, see: (a) Hewes, J. D.; Kreimendahl, C. W.; Marder, T. B.; Hawthorne, M. F. Metal-Promoted Insertion of an Activated Alkene into a B−H Bond of an Exopolyhedra *nido*-Rhodacarboran-Rhodium-Catalyzed Hydroboration. *J. Am. Chem. Soc.* **1984**, *106*, 5757−5759. (b) Sun, F. X.; Tan, S. M.; Cao, H. J.; Xu, J. K.; Bregadze, V. I.; Tu, D. S.; Lu, C. S.; Yan, H. Palladium-Catalyzed Hydroboration of Alkynes with Carboranes: Facile Construction of a Library of Boron Cluster-Based AIE-Active Luminogens. *Angew. Chem., Int. Ed.* **2022**, *61*, No. e202207125. (c) Sun, F. X.; Tan, S. M.; Cao, H. J.; Lu, C. S.; Tu, D. S.; Poater, J.; Sola, M.; Yan, H. Facile Construction of New Hybrid Conjugation via Boron Cage Extension. *J. Am. Chem. Soc.* **2023**, *145*, 3577−3587. (d) Li, P.; Yang, J.; Zeng, J.; Miao, S.; Fang, R.; Lu, J.; Lu, J. Y. Regiocontrollable B(2/3)−H Alkenylation of *nido*-Carboranes. *Org. Lett.* **2024**, *26*, 8134−8138. (e) Sun, Z.; Zong, J.;

https://doi.org/10.1021/jacs.5c01610
J. Am. Chem. Soc. 2025, 147, 12845−12857

Ren, H.; Lu, C. S.; Tu, D. S.; Poater, J.; Solà, M.; Shi, Z. Z.; Yan, H. Couple-Close Construction of Non-classical Boron Cluster-phosphonium Conjugates. *Nat. Commun.* **2024**, *15*, 7934.

(13) For selected reviews and references of the photoredox catalysis, see: (a) Tian, Y. M.; Guo, X. N.; Braunschweig, H.; Radius, U.; Marder, T. B. Photoinduced Borylation for the Synthesis of Organoboron Compounds. *Chem. Rev.* **2021**, *121*, 3561−3597. (b) Chang, L.; An, Q.; Duan, L.; Feng, K.; Zuo, Z. W. Alkoxy Radicals See the Light: New Paradigms of Photochemical Synthesis. *Chem. Rev.* **2022**, *122*, 2429−2486. (c) Wang, P. Z.; Zhang, B.; Xiao, W. J.; Chen, J. R. Photocatalysis Meets Copper Catalysis: A New Opportunity for Asymmetric Multicomponent Radical Cross-Coupling Reactions. *Acc. Chem. Res.* **2024**, *57*, 3433−3448. (d) Chan, A. Y.; Perry, I. B.; Bissonnette, N. B.; Buksh, B. F.; Edwards, G. A.; Frye, L. I.; Garry, O. L.; Lavagnino, M. N.; Li, B. X.; Liang, Y.; Mao, E.; Millet, A.; Oakley, J. V.; Reed, N. L.; Sakai, H. A.; Seath, C. P.; MacMillan, D. W. C. Metallaphotoredox: The Merger of Photoredox and Transition Metal Catalysis. *Chem. Rev.* **2022**, *122*, 1485−1542. (e) Hu, A. H.; Guo, J. J.; Pan, H.; Zuo, Z. W. Selective Functionalization of Methane, Ethane, and Higher Alkanes by Cerium Photocatalysis. *Science* **2018**, *361*, 668−672. (f) Wen, L.; Ding, J.; Duan, L. F.; Wang, S.; An, Q.; Wang, H. X.; Zuo, Z. W. Multiplicative Enhancement of Stereoenrichment by a Single Catalyst for Deracemization of Alcohols. *Science* **2023**, *382*, 458−464. (g) Lei, T.; Cheng, Y. Y.; Han, X.; Zhou, C.; Yang, B.; Fan, X. W.; Chen, B.; Tung, C. H.; Wu, L. Z. Lewis Acid-Relayed Singlet Oxygen Reaction with Enamines: Selective Dimerization of Enamines to Pyrrolin-4-ones. *J. Am. Chem. Soc.* **2022**, *144*, 16667−16675. (h) Chang, L.; Wang, S.; An, Q.; Liu, L.; Wang, H.; Li, Y.; Feng, K.; Zuo, Z. W. Resurgence and Advancement of Photochemical Hydrogen Atom Transfer Processes in Selective Alkane Functionalizations. *Chem. Sci.* **2023**, *14*, 6841−6859. (i) Liu, W. Q.; Lei, T.; Zhou, S.; Yang, X. L.; Li, J.; Chen, B.; Sivaguru, J.; Tung, C. H.; Wu, L. Z. Cobaloxime Catalysis: Selective Synthesis of Alkenylphosphine Oxides under Visible Light. *J. Am. Chem. Soc.* **2019**, *141*, 13941−13947.

(14) For selected references for preactivation of B−H bonds, see: (a) Zhao, D.; Xie, Z. W. Visible-Light-Promoted Photocatalytic B−C Coupling via a Boron-Centered Carboranyl Radical: Facile Synthesis of B(3)-Arylated *o*-Carboranes. *Angew. Chem., Int. Ed.* **2016**, *55*, 3166−3170. (b) Chen, M.; Xu, J. K.; Zhao, D. S.; Sun, F. X.; Tian, S. M.; Tu, D. S.; Lu, C. S.; Yan, H. Site-Selective Functionalization of Carboranes at the Electron-Rich Boron Vertex: Photocatalytic B−C Coupling via a Carboranyl Cage Radical. *Angew. Chem., Int. Ed.* **2022**, *61*, No. e202205672. (c) Li, S. M.; Xie, Z. W. Visible-Light-Promoted Nickel-Catalyzed Cross-Coupling of Iodocarboranes with (Hetero)-Arenes via Boron-Centered Carboranyl Radicals. *J. Am. Chem. Soc.* **2022**, *144*, 7960−7965.

(15) Ren, H. Y.; Zhang, P.; Xu, J. K.; Ma, W. L.; Tu, D. S.; Lu, C. S.; Yan, H. Direct B−H Functionalization of Icosahedral Carboranes via Hydrogen Atom Transfer. *J. Am. Chem. Soc.* **2023**, *145*, 7638−7647.

(16) Gruzdev, D. A.; Levit, G. L.; Krasnov, V. P.; Charushin, V. N. Carborane-containing amino acids and peptides: Synthesis, properties and applications. *Coord. Chem. Rev.* **2021**, *433*, No. 213753.

(17) For selected references of near-infrared (NIR) light advantages and catalysis, see: (a) Ravetz, B. D.; Pun, A. B.; Churchill, E. M.; Congreve, D. N.; Rovis, T.; Campos, L. M. Photoredox Catalysis Using Infrared Light via Triplet Fusion Upconversion. *Nature* **2019**, *565*, 343−346. (b) Cabanero, D. C.; Rovis, T. Low-energy Photoredox Catalysis. *Nat. Rev. Chem.* **2025**, *9*, 28−45.

(18) (a) Xu, S. W.; Zhang, H. J.; Xu, J. K.; Suo, W. Q.; Lu, C. S.; Tu, D. S.; Guo, X. W.; Poater, J.; Sola, M.; Yan, H. Photoinduced Selective B−H Activation of *nido*-Carboranes. *J. Am. Chem. Soc.* **2024**, *146*, 7791−7802. (b) Tu, D. S.; Yan, H.; Poater, J.; Solà, M. The *nido*-Cage···π Bond: A Non-covalent Interaction between Boron Clusters and Aromatic Rings and Its Applications. *Angew. Chem., Int. Ed.* **2020**, *59*, 9018−9025. (c) Fu, M. C.; Shang, R.; Zhao, B.; Wang, B.; Fu, Y. Photocatalytic Decarboxylative Alkylations Mediated by Triphenylphosphine and Sodium Iodide. *Science* **2019**, *363*, 1429−1434. (d) Arceo, E.; Jurberg, I. D.; Álvarez-Fernández, A.; Melchiorre, P. Photochemical Activity of a Key Donor-acceptor Complex Can Drive Stereoselective Catalytic α-Alkylation of Aldehydes. *Nat. Chem.* **2013**, *5*, 750−756.

(19) For selected reviews of oligopeptide, see: (a) Lee, A. C. L.; Harris, J. L.; Khanna, K. K.; Hong, J. H. A Comprehensive Review on Current Advances in Peptide Drug Development and Design. *Int. J. Mol. Sci.* **2019**, *20*, 2383. (b) Varanko, A.; Saha, S.; Chilkoti, A. Recent Trends in Protein and Peptide-based Biomaterials for Advanced Drug Delivery. *Adv. Drug Deliver. Rev.* **2020**, *156*, 133−187. (c) Muttenthaler, M.; King, G. F.; Adams, D. J.; Alewood, P. F. Trends in Peptide Drug Discovery. *Nat. Rev. Drug. Disc.* **2021**, *20*, 309−325.

(20) (a) Hosmane, N. S.; Maguire, J. A.; Zhu, Y.; Takagaki, M. Future Perspectives for Boron and Gadolinium Neutron Capture Therapies in Cancer Treatment. *InBoron and Gadolinium Neutron Capture Therapy for Cancer Treatment*; World Scientific: Singapore, 2011; pp 165170. (b) Sauerwein, W.; Wittig, A.; Moss, R.; Nakagawa, Y. *Neutron Capture Therapy*; Springer Science & Business Media, 2012. (c) Zhu, Y.; Peng, A. T.; Carpenter, K.; Maguire, J. A.; Hosmane, N. S.; Takagaki, M. Substituted Carborane-Appended Water-Soluble Single-Wall Carbon Nanotubes: New Approach to Boron Neutron Capture Therapy Drug Delivery. *J. Am. Chem. Soc.* **2005**, *127*, 9875−9880. (d) Hawthorne, M. F. The Role of Chemistry in the Development of Boron Neutron Capture Therapy of Cancer. *Angew. Chem., Int. Ed.* **1993**, *32*, 950−984. (e) Alamón, C.; Dávila, B.; García, M. F.; Nievas, S.; Dagrosa, M. A.; Thorp, S.; Kovacs, M.; Trias, E.; Faccio, R.; Gabay, M.; Zeineh, N.; Weizman, A.; Teixidor, F.; Viñas, C.; Gavish, M.; Cerecetto, H.; Couto, M. A Potential Boron Neutron Capture Therapy Agent Selectively Suppresses High-Grade Glioma. *In Vitro and in Vivo Exploration. Mol. Pharmaceut.* **2023**, *20*, 2702−2713. (f) Coghi, P.; Li, J.; Hosmane, N. S.; Zhu, Y. Next Generation of Boron Neutron Capture Therapy (BNCT) Agents for Cancer Treatment. *Med. Res. Rev.* **2023**, *43*, 1809−1830. (g) Zhang, X.; Lin, Y.; Hosmane, N. S.; Zhu, Y. Nanostructured Boron Agents for Boron Neutron Capture Therapy: A Review of Recent Patents. *Med. Rev.* **2023**, *3*, 425−443.

(21) (a) Cheng, X.; Li, F.; Liang, L. Boron Neutron Capture Therapy: Clinical Application and Research Progress. *Curr. Oncol.* **2022**, *29*, 7868−7886. (b) Soloway, A.; Tjarks, W.; Barnum, B.; Rong, F.; Barth, R.; Codogni, I.; Wilson, J. The Chemistry of Neutron Capture Therapy. *Chem. Rev.* **1998**, *98*, 1515−1562.

(22) Ruhlmann, M.; Jentzen, W.; Ruhlmann, V.; Pettinato, C.; Rossi, G.; Binse, I.; Bockisch, A.; Rosenbaum-Krumme, S. High Level of Agreement Between Pretherapeutic ^{124}I PET and Intratherapeutic ^{131}I Imaging in Detecting Iodine-Positive Thyroid Cancer Metastases. *J. Nucl. Med.* **2016**, *57*, 1339−1342.

(23) For selected references of aggregation-induced emission (AIE): (a) Zhu, F. Y.; Mei, L. J.; Tian, R.; Li, C.; Wang, Y. L.; Xiang, S. L.; Zhu, M. Q.; Tang, B. Z. Recent Advances in Super-Resolution Optical Imaging Based on Aggregation-Induced Emission. *Chem. Soc. Rev.* **2024**, *53*, 3350−3383. (b) Mei, J.; Leung, N. L. C.; Kwok, R. T. K.; Lam, J. W. Y.; Tang, B. Z. Aggregation-Induced Emission: Together We Shine, United We Soar! *Chem. Rev.* **2015**, *115*, 11718−11940. (c) Zhang, X.; Wang, K.; Gao, Z.; Wu, Z.; Liu, W.; Li, J.; Gao, H.; Wei, J.; Ding, D.; Zheng, W. An Aggre-gation-Induced Emission Molecule-Assembled Nanovaccine with Self-Adjuvanted Function for Cancer Immunotherapy. *Adv. Funct. Mater.* **2023**, *33*, No. 2302118. (d) Ji, S.; Pan, T.; Wang, K.; Zai, W.; Jia, R.; Wang, N.; Jia, S.; Ding, D.; Shi, Y. A Membrane-Anchoring Self-Assembling Peptide Allows Bioorthogonal Coupling of Type-I AIEgens for Pyroptosis-Induced Cancer Therapy. *Angew. Chem., Int. Ed.* **2024**, *64*, No. e202415735. (e) Ma, W. L.; Wang, Y. Y.; Xue, Y. L.; Wang, M. M.; Lu, C. S.; Guo, W. H.; Liu, Y. H.; Shu, D. Y.; Shao, G. Q.; Xu, Q. F.; Tu, D. S.; Yan, H. Molecular Engineering of AIE-active Boron Clustoluminogens for Enhanced Boron Neutron Capture Therapy. *Chem. Sci.* **2024**, *15*, 4019−4030. (f) Chen, J.; Chen, L.; She, Z.; Zeng, F.; Wu, S. A Multifunctional Nanoaggregate-based System for Detection of Rheumatoid Arthritis via Optoacoustic/NIR-II Fluorescent Imaging and Therapy via Inhibiting JAK-STAT/NF-κB/NLRP3 Pathways. *Aggregate* **2024**, *5*, No. e419. (g) Shimoyama, D.; Jäkle, F. Controlling

https://doi.org/10.1021/jacs.5c01610
J. Am. Chem. Soc. 2025, 147, 12845−12857

the Aggregation and Assembly of Boron-Containing Molecular and Polymeric Materials. *Aggregate* **2022**, *3*, No. e149. (h) Wada, K.; Hashimoto, K.; Ochi, J.; Tanaka, K.; Chujo, Y. Rational Design for Thermochromic Luminescence in Amorphous Polystyrene Films with Bis-*o*-Carborane-Substituted Enhanced Conjugated Molecule Having Aggregation-induced Luminochromism. *Aggregate* **2021**, *2*, No. e93.
(24) Brezová, V.; Pigošová, J.; Havlínová, B.; Dvoranová, D.; Ďurovič, M. EPR Study of Photochemical Transformations of Triarylmethane Dyes. *Dyes Pigments* **2004**, *61*, 177−198.

https://doi.org/10.1021/jacs.5c01610
J. Am. Chem. Soc. 2025, 147, 12845−12857